ELSEVIER

Journal of Power Sources 101 (2001) 275–286

JOURNAL OF POWER SOURCES

www.elsevier.com/locate/jpowsour

Modeling polymer electrolyte fuel cells: an innovative approach

G. Maggio*, V. Recupero, L. Pino

CNR-TAE Institute, Via Salita S., Lucia sopra Contesse 5, 98126 Santa Lucia, Messina, Italy

Received 18 December 2000; received in revised form 2 March 2001; accepted 5 March 2001

Abstract

In this paper, a mathematical simulation model is proposed to describe the water transport in proton conductive membranes, used in polymer electrolyte fuel cells (PEFCs). The model, which includes the calculation of electrochemical parameters of a PEFC, represents a quite innovative approach. In fact, it is based on the use of original mathematical relationships taking into account diffusional and ohmic overpotentials for electrode flooding and membrane dehydration problems.

The calculated performance of polymer fuel cells using a Nafion 117 membrane clearly demonstrates the model validation (±3% variation with respect to experimental data). Besides, analysis of model results allows a useful comparison of two different membranes (Nafion 117, Dow) in order to define the best membrane/electrode assembly.

Keywords: Electrode flooding; Membrane dehydration; Modeling; Polymer electrolyte fuel cells; Water transport

1. Introduction

The polymer electrolyte fuel cell (PEFC) operates at a low temperature (70–90°C), and promises to be one of the most serious candidates for both stationary and automotive applications as a substitute of traditional systems (thermoelectric power plants, internal combustion engine, etc.), due to well-known advantages (high efficiency, no pollutant emission, etc.).

The stringent requirements in terms of compactness, high energy density, performance stability and low cost, move the R&D in the direction of optimizing the different aspects of the PEFC systems. One approach is the development of theoretical analysis in order to identify and to solve problems related with the above-mentioned items.

In this respect, several mathematical models have been proposed in literature for PEFCs [1–25]; all these models aimed at determining the potential or cell voltage as a function of the current density and, in general, of the operating conditions.

One of the key objectives of the current research is an adequate water content in the electrolyte to achieve a good ionic conductivity. In fact, membrane dehydration causes an increase in resistance to the proton flow (the ionic charges move through the sulfonic groups of the polymeric membrane surrounded by water molecules) and possible deadhesion of the membrane from the electrode. On the other hand, for excess water content, the cathode is flooded and the diffusion of the reactant gas through its pores is hindered. Therefore, an accurate evaluation of the water transport in PEFCs, often made by modeling approaches [1–5], is desirable. Nevertheless, a formulation that directly relates the performance of a polymer fuel cell with the cathode flooding and/or the dehydration problems at the membrane/electrode interfaces has never been proposed.

As evidenced in literature [11], the cathode flooding, typical of high current density operation, involves a decrease in the porosity available for gas diffusion in the electrode. Likely, it can be inferred that the membrane dehydration phenomenon, that especially occurs on the anode side at high current densities, involves a decrease in ionic conductivity [7–9,11,26].

Starting from these considerations, a mathematical model has been developed. It has been validated and applied to polymer fuel cells based on Nafion 117 and Dow membranes.

2. Model development

In this paragraph, a description of the mathematical model developed for the solid polymer electrolyte fuel cell is presented. The main assumptions of the model are: (i) one-dimensional treatment; (ii) isothermal and steady state

* Corresponding author. Tel.: +39-90-624227; fax: +39-90-624247.
E-mail address: maggio@itae.me.cnr.it (G. Maggio).

0378-7753/01/$ – see front matter
PII: S0378-7753(01)00758-3

Nomenclature

A	superficial electrode area (cm^2)
c_{H^+}	fixed-charge concentration (mol cm^{-3})
d	membrane average pore diameter (cm)
$\mathscr{D}_{H^+}$	protonic diffusion coefficient ($cm^2\ s^{-1}$)
$D_{O_2N_2}$	oxygen/nitrogen binary diffusion coefficient at standard conditions ($cm^2\ s^{-1}$)
EW	membrane equivalent weight (g mol^{-1})
F	Faraday constant (96,487 C per eq.)
I	current density (A cm^{-2})
I_{lim}	limiting current density (A cm^{-2})
I_o	exchange current density (A cm^{-2})
$I_{o,Pt}$	exchange current density per Pt surface (A cm^{-2} Pt)
k_p	membrane hydraulic permeability (cm^2)
k_Φ	membrane electrokinetic permeability (cm^2)
l_{d+}	cathode gas-diffusion layer thickness (cm)
l_m	wet membrane thickness (cm)
M	water amount to be added to the cell (mol s^{-1})
$M_{1,max}$	water amount corresponding to complete flooding (mol s^{-1})
$M_{2,max}$	water amount corresponding to complete dehydration (mol s^{-1})
OCV	open circuit voltage (V)
p	gas pressure (atm)
p_w^{sat}	saturated vapor pressure (atm)
R	universal gas constant (8.3143 J $mol^{-1}\ K^{-1}$)
R_{cell}	cell resistance ($\Omega\ cm^2$)
R_{memb}	membrane resistance ($\Omega\ cm^2$)
S_{Pt}	catalyst surface area ($cm^2\ mg^{-1}$)
T	cell temperature (K)
U_{Pt}	catalyst utilization
v	water velocity in membrane pores (cm s^{-1})
V_{cell}	cell voltage (V)
V_m	standard molar volume (22,414 $cm^3\ mol^{-1}$)
W	water flow rate (mol $cm^{-2}\ s^{-1}$)
W_{Pt}	catalyst loading (mg cm^{-2})
x	gas-phase mole fraction

Greek symbols

δ	pore-water density (mol cm^{-3})
δ_{dry}	membrane dry density (g cm^{-3})
ε_g^d	gas porosity in gas-diffusion layer
ε_w^m	membrane water porosity
η	cell overpotential (V)
κ	membrane ionic conductivity ($\Omega^{-1}\ cm^{-1}$)
μ	pore-water viscosity (kg $m^{-1}\ s^{-1}$)
τ_R	membrane resistance/cell resistance ratio
ω	empirical constant for diffusional overpotential ($\Omega\ cm^2\ K^{-1}$)
ξ	membrane water-transport ratio
ζ	stoichiometric ratio

Subscripts and superscripts

act	activation
conv	convective
dif	diffusional
el	electrochemical reaction
in	cell inlet
o	initial or inlet to gas chamber
ohm	ohmic
out	cell outlet
sat	saturated condition
tr	water transport
um	humidification condition
w	water
+	cathode side
−	anode side

conditions; (iii) ideal and uniformly distributed gases; (iv) electrode pores for gas flow are separated from pores for liquid water; (v) the inlet gas temperatures are equal to the cell temperature.

A set of input data is used for model calculations that, for convenience, have been divided into two distinct sections: water balance calculations and electrochemical calculations. It must be remarked that the gas porosity in the cathode diffusional layer and the ionic conductivity of the membrane, which affect diffusional and ohmic overpotentials, strictly depend on the water balance conditions calculated at any current density value. The core of the calculations is preceded by the determination of the membrane properties.

2.1. Membrane properties calculations

To calculate the membrane properties, the following equations have been used:

$$c_{H^+} = \frac{\delta_{dry}(1-\varepsilon_w^m)}{EW}, \tag{1}$$

$$k_\Phi = \frac{\varepsilon_w^m d^2}{80}, \tag{2}$$

$$\mu = 1.002 \times 10^{(((1.3272(293-T)-0.001053(293-T)^2)/(T-168))-3}, \tag{3}$$

$$\delta = 3.014 \times 10^{-2} + 2.216 \times 10^{-4}T - 5.842 \times 10^{-7}T^2 + 4.179 \times 10^{-10}T^3, \tag{4}$$

$$\mathscr{D}_{H^+} = \mathscr{D}_{H^+(22^\circ C)} \frac{T}{\mu} \frac{\mu_{(22^\circ C)}}{295}, \tag{5}$$

$$\kappa^o = \frac{F^2}{RT} \mathscr{D}_{H^+} c_{H^+}, \tag{6}$$

where $\mu_{(22^\circ C)} = 0.9548 \times 10^{-3}$ kg $m^{-1}\ s^{-1}$ is the water viscosity at 22°C. In particular, the equations for fixed-charge concentration (Eq. (1)), electrokinetic permeability (Eq. (2)), and initial ionic conductivity (Eq. (6)) have already been reported in literature [2,27]. The equations for pore-water viscosity (Eq. (3)) and density (Eq. (4)) have been obtained by extrapolation of data reported in [28], in the

proper ranges of temperature (20–100 and 40–100°C, respectively). Finally, the protonic diffusion coefficient (Eq. (5)) has been derived on the basis of the relationship $\mathscr{D}\mu/T = \text{constant}$ [2].

At the first calculation loop, corresponding to OCV conditions, it will be

$$\kappa = \kappa^{\mathrm{o}}. \tag{7}$$

2.2. Water balance equations

The model makes a set of calculations in order to verify on the basis of fixed experimental conditions, the water transport characteristics of the membrane and to suggest some solutions in order to achieve an optimal water transport in the fuel cell.

As already mentioned, a proper water balance is critical for good operation of a polymer fuel cell, also during transient response. It is necessary to identify operative conditions able to avoid electrode flooding and membrane dehydration problems which can drastically reduce the cell performance.

In particular, at low current density, dehydration of the cathode side of the membrane can occur: the water produced within the cathode and that dragged through the membrane from the anode to the cathode due to electro-osmosis (with H^+ protons) could be insufficient. On the contrary, at high current density, the water production at the cathode can cause a flooding of the electrode. Moreover, the electro-osmotic flow of water increases with current, and the anode side of the membrane is thus subjected to dehydration, which is only partially counterbalanced by *back diffusion* (from cathode to anode). Then, with the exception of the intermediate current density region, at low and high current densities, a proper water balance can be obtained only by using appropriate expedients, e.g. by humidification of the gases entering the fuel cell or by supplying (removing) liquid water.

Fig. 1 outlines the water flows inside the cell. According to [29], the amount of water produced by chemical reaction due to cross-over of gases can be neglected.

The following equations have been used to determine the water flow rates related to the different phenomena:

$$\text{Water transport}: \qquad W_{\mathrm{tr}} = \frac{I}{F}\xi. \tag{8}$$

$$\text{Electrochemical reaction}: \qquad W_{\mathrm{el}} = \frac{I}{2F}. \tag{9}$$

$$\text{Anode humidification}: \qquad W_{-}^{\mathrm{um}} = \frac{I}{2F}\zeta_{-}\frac{x_{\mathrm{w}}^{\mathrm{um}-}}{1-x_{\mathrm{w}}^{\mathrm{um}-}}. \tag{10}$$

Cathode humidification :

$$W_{+}^{\mathrm{um}} = \frac{I}{4F}\zeta_{+}\frac{x_{\mathrm{w}}^{\mathrm{um}+}}{1-x_{\mathrm{w}}^{\mathrm{um}+}}\left(1+\frac{x_{\mathrm{N_2}}^{\mathrm{o}}}{x_{\mathrm{O_2}}^{\mathrm{o}}}\right). \tag{11}$$

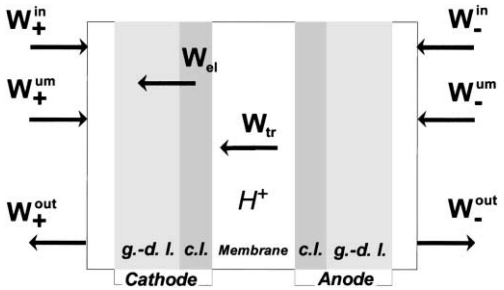

Fig. 1. Schematic of water balance model — g.-d.l.: gas-diffusion layer; c.l.: catalyst layer; W_{-}^{um}, W_{+}^{um}: water entering the cell due to fuel and oxidant humidification, respectively; W_{-}^{in}, W_{+}^{in}: water directly added (e.g. by wicking) to the anode and cathode compartment, respectively; W_{el}: water produced in the cell (on the cathode side) from the electrochemical reaction; W_{tr}: water transported through the membrane from anode to cathode due to drag (electro-osmosis) and diffusion (or back diffusion) phenomena; W_{-}^{out}, W_{+}^{out}: water outgoing from anode and cathode compartment, respectively.

$$\text{Anode outlet}: \qquad W_{-}^{\mathrm{out}} = \frac{I}{2F}(\zeta_{-}-1)\frac{x_{\mathrm{w}}^{\mathrm{sat}-}}{1-x_{\mathrm{w}}^{\mathrm{sat}-}}. \tag{12}$$

Cathode outlet :

$$W_{+}^{\mathrm{out}} = \frac{I}{4F}\left[\zeta_{+}\left(1+\frac{x_{\mathrm{N_2}}^{\mathrm{o}}}{x_{\mathrm{O_2}}^{\mathrm{o}}}\right)-1\right]\frac{x_{\mathrm{w}}^{\mathrm{sat}+}}{1-x_{\mathrm{w}}^{\mathrm{sat}+}}. \tag{13}$$

According to [1,3,4], the membrane water-transport ratio can be calculated as

$$\xi = \varepsilon_{\mathrm{w}}^{\mathrm{m}} F\frac{\delta v}{I}, \tag{14}$$

where v is the water velocity in the membrane pores, determined by the following equation:

$$v = \left[\frac{k_{\Phi}c_{\mathrm{H^+}}FI}{\mu k}-\frac{k_{\mathrm{p}}}{\mu}\frac{\mathrm{d}p}{\mathrm{d}z}\right]\left(1+\frac{F^2c_{\mathrm{H^+}}^2k_{\Phi}}{\mu k}\right)^{-1}, \tag{15}$$

which establishes that the water transport in the membrane depends on two contributions: the electro-osmotic transport associated with the flow of the H^+ protons, and the diffusive transport due to a pressure gradient in the membrane ($\mathrm{d}p/\mathrm{d}z$). This last term can be obtained by known relationships [1,3,4].

The gas-phase mole fractions of water corresponding to saturated condition have been calculated as

$$x_{\mathrm{w}}^{\mathrm{sat}-} = \frac{p_{\mathrm{w}}^{\mathrm{sat}}}{p_{-}}, \tag{16}$$

$$x_{\mathrm{w}}^{\mathrm{sat}+} = \frac{p_{\mathrm{w}}^{\mathrm{sat}}}{p_{+}}, \tag{17}$$

with

$$p_{\mathrm{w}}^{\mathrm{sat}} = \exp\left(13.669-\frac{5096.23}{T}\right). \tag{18}$$

Analogously, the mole fractions of water corresponding to humidification condition ($x_{\mathrm{w}}^{\mathrm{um}-}$, $x_{\mathrm{w}}^{\mathrm{um}+}$) can be determined by

considering the humidification temperatures, instead of the cell temperature in Eq. (18).

The water balance is expressed by the following relationships:

$$\text{At the anode :} \qquad W_{-}^{\text{out}} = W_{-}^{\text{in}} + W_{-}^{\text{um}} - W_{\text{tr}}, \tag{19}$$

$$\text{At the cathode :} \qquad W_{+}^{\text{out}} = W_{+}^{\text{in}} + W_{+}^{\text{um}} + W_{\text{el}} + W_{\text{tr}}. \tag{20}$$

The amounts of water to be supplied at the anode and at the cathode compartment to achieve the water balance are

$$M_{-} = W_{-}^{\text{in}} A, \tag{21}$$

$$M_{+} = W_{+}^{\text{in}} A. \tag{22}$$

It is evident that when these last equations give negative values, a removal, instead of addition, of the corresponding water amounts is required to obtain the balance.

2.3. Electrochemical calculation equations

As well known [30,31], under operative conditions, the voltage of a fuel cell decreases, compared with the ideal or reversible theoretical value, because of the irreversible losses associated with activation, ohmic, and diffusional polarizations. Once estimated accurately such effects, it is possible to obtain a sufficiently correct description of the cell performance.

Cell voltage can be determined by subtracting the overpotentials related to the cell irreversibilities from the open circuit voltage (OCV),

$$V_{\text{cell}} = \text{OCV} - \eta_{\text{act}} - \eta_{\text{ohm}} - \eta_{\text{dif}} - \eta_{\text{conv}}, \tag{23}$$

where η_{act} is the activation overpotential, η_{ohm} the ohmic overpotential, and η_{dif} the diffusional overpotential; the last term η_{conv} has been introduced on the basis of the following considerations.

The flux of a dissolved species in the membrane pores is due to three effects: migration, diffusion, and convection [2,32,33]. The first one corresponds to the ohmic term related to the membrane (already included in η_{ohm}), the second is associated with the so-called diffusion potential, and the third to the effect of the potential gradient on the velocity of the charged fluid. In the case of a PEFC, the only mobile ions in the membrane pores are hydrogen ions, whose concentration in the membrane is constant; thus, there is no proton transport due to diffusion [2,33]. Therefore, only the proton transport for convection, to which the overpotential η_{conv} is associated, has to be considered.

The OCV has been calculated by using the following equation [1–4]:

$$\text{OCV} = 1.23 - 0.9 \times 10^{-3}(T - 298) + \frac{RT}{4F} \ln(p_{\text{H}_2}^2 p_{\text{O}_2}). \tag{24}$$

To calculate the different overpotentials, the following relationships have been considered:

$$\text{Activation overpotential :} \qquad \eta_{\text{act}} = \frac{RT}{F} \ln\left(\frac{I}{I_{\text{o}}}\right). \tag{25}$$

$$\text{ohmic overpotential :} \qquad \eta_{\text{ohm}} = IR_{\text{cell}}. \tag{26}$$

$$\text{Diffusional overpotential :} \qquad \eta_{\text{dif}} = \omega TI \ln\left(\frac{I_{\text{lim}}}{I_{\text{lim}} - I}\right). \tag{27}$$

$$\text{Convective overpotential :} \qquad \eta_{\text{conv}} = Fc_{\text{H}^+} v \frac{l_{\text{m}}}{\kappa}. \tag{28}$$

In Eq. (26), the cell resistance is considered to vary as a function of the current density, depending on the water balance conditions.

Eq. (27) for diffusional overpotential is different from that commonly reported in most handbooks on fuel cells [30,31]. Here, the pre-logarithmic term is assumed to be dependent on current density, according to [16,34], whose purpose was to simulate the cell behavior in the entire current density region through a rational description of mass-transport problems. Moreover, unlike the classical approaches, the limiting current density (I_{lim}) varies as a function of the cell current density, and decreases in consequence of the flooding of the cathode gas-diffusion layer (see Eq. (31)).

Eq. (28) provides the overpotential associated with proton convection, which depends on the protonic concentration and water velocity in the membrane pores [1–4].

Exchange current density per geometrical electrode surface, cell resistance, and limiting current density have been determined by the following equations:

$$I_{\text{o}} = I_{\text{o,Pt}} S_{\text{Pt}} W_{\text{Pt}} U_{\text{Pt}}, \tag{29}$$

$$R_{\text{cell}} = \frac{R_{\text{memb}}}{\tau_{\text{R}}} = \frac{l_{\text{m}}}{\kappa \tau_{\text{R}}}, \tag{30}$$

$$I_{\text{lim}} = -\frac{2FD_{\text{O}_2\text{N}_2}(\varepsilon_{\text{g}}^{\text{d}})^{1.5}(T/273)^{0.823}}{V_{\text{m}} l_{\text{d}+}} \ln(1 - x_{\text{O}_2}), \tag{31}$$

where $I_{\text{o,Pt}}$ is the exchange current density referred to Pt surface, S_{Pt} the catalyst surface area, W_{Pt} the catalyst loading in the electrode, U_{Pt} the catalyst utilization coefficient, $\tau_{\text{R}} \leq 1$ the membrane resistance/cell resistance ratio, assumed to be constant (Eq. (31) from [11]).

Eq. (31) gives the dependency of the limiting current on the gas porosity in the cathode diffusional layer, in agreement with the results obtained in [1–4] and with the considerations explained in [11]: gas transport limitations in the cathode diffusional layer determine the limiting current of the cell.

Finally, the gas porosity in the cathode diffusional layer and the membrane ionic conductivity have been determined from the following expressions:

$$\varepsilon_{\text{g}}^{\text{d}} = \varepsilon_{\text{g}}^{\text{d,o}} \left(1 - \frac{|M_{+}|}{M_{1,\text{max}}}\right), \quad \text{if } M_{+} < 0, \tag{32}$$

$$\kappa = \begin{cases} \kappa^{o}\left(1 - \dfrac{M_{+,-}}{M_{2,\max}}\right), & \text{if } M_{+,-} > 0 \text{ and } M_{-,+} \leq 0, \\ \kappa^{o}\left(1 - \dfrac{M_{+}}{M_{2,\max}}\right)\left(1 - \dfrac{M_{-}}{M_{2,\max}}\right), & \text{if } M_{+} > 0 \text{ and } M_{-} > 0, \end{cases} \tag{33}$$

being $\varepsilon_g^{d,o}$ the initial porosity in the gas-diffusion layer, κ^o the initial membrane ionic conductivity calculated by Eq. (6), M_+ and M_- the amounts of water required for water balance on the cathode and on the anode side, respectively, derived from previous calculations (Eqs. (21) and (22)), $M_{1,\max}$ the water amount corresponding to a complete flooding, and $M_{2,\max}$ the water deficit corresponding to complete dehydration. As a first approximation, it has been assumed

$$M_{2,\max} = M_{1,\max}, \tag{34}$$

that is, the water deficit that results in complete dehydration at the membrane/electrode interfaces is equal to the excess water amount that induces the complete flooding of the cathode gas-diffusion layer.

3. Innovative aspects of the proposed model

All the mathematical models for polymer fuel cells so far proposed assume the gas porosity in the electrode diffusional layer to be constant (for example, 40% in [1–4]). Nevertheless, Springer et al. [11] have previously evidenced that this assumption does not explain the limiting current experimentally obtained and their dependence on gas composition and pressure. As was observed, the average effective porosity of the gas-diffusion layer should be significantly lower (from 25 to 18.6% between 0 and 1.5 A cm^{-2} in [11]) than the ''natural'' porosity (ca. 40%) of the carbon cloth electrode. The reason is a noticeable ''partial flooding'' of the cathode by the liquid water produced that slows down the oxygen transport.

To express such an effect, we assumed that the gas porosity in the diffusional layer decreases, in case of cathode flooding ($M_+ < 0$), according to Eq. (32). In other words, it is assumed that the gas porosity in the diffusional layer depends on current density; it decreases when the latter increases, in agreement with [11].

In the mathematical model presented in [11], the effective porosity (liquid water-free pores) could be ''adjusted'' and was considered either independent from the current density or decreased in proportion to the rate of water production at the cathode. To obtain reliable values of the effective porosities corresponding to a given fuel cell, the authors were forced to realize a simultaneous fitting of several polarization curves of the cell [11] recorded under different operative conditions. Our approach, differently, allows direct calculation of the gas porosity through Eq. (32).

As the cathode flooding involves a decrease in the porosity available for the gas that diffuses through the electrode, it can be argued that the membrane dehydration involves a decrease in ionic conductivity. As a consequence, the overall cell resistance, to which the membrane strongly contributes, will correspondingly increase.

Even though such an effect is neglected in mathematical models for fuel cells (except [9]), where a constant resistance is considered, it is evidenced in some experimental works [7,8,11,26]: e.g. a resistance increase in the order of 10% going from 0 to 0.8 A cm^{-2} for a cell based on Nafion 117 is observed in [26].

Therefore, in analogy with the method used for the gas porosity, we assumed that the membrane ionic conductivity decreases, in case of cathode ($M_+ > 0$) and/or anode dehydration ($M_- > 0$), according to Eq. (33). Eq. (33) is equivalent to the assumption that the ionic conductivity of the membrane depends on current density, by decreasing when the latter increases, in agreement with [26]. A decrease in the membrane ionic conductivity and thus an increase in the cell resistance at low current densities due to the incidental dehydration at membrane/cathode interface ($M_+ > 0$) is also expected from Eq. (33).

The innovative character of the proposed model is evident. In particular, the more original aspect consists in the correlation introduced between the performance of the polymer fuel cell and the water balance conditions. In fact, although it is evident that possible problems of electrode flooding and/or membrane/electrodes dehydration cannot be uninfluential on the operation of this type of fuel cell, no literature model explicitly expresses this. Such a result has been obtained here through the use of two mathematical relationships (Eqs. (32) and (33)) which state that the gas porosity in the cathode diffusional layer and the membrane conductivity vary with the current density, in agreement with some literature considerations [11,26]. As a consequence, the diffusional (Eq. (27)) and ohmic overpotentials (Eq. (26)) increase in case of flooding and dehydration problems, respectively.

This effect is shown, from a qualitative point of view, in Figs. 2 and 3, where the overpotentials are reported in arbitrary unities (A.U.). In particular, in Fig. 3 the membrane/cathode dehydration problems have been emphasized. Appropriate humidification conditions would let us exclude the occurrence of this phenomenon. Nevertheless, as already mentioned, if the humidification conditions are not adequate, at low current densities, the water produced at the cathode and that dragged from anode to cathode due to

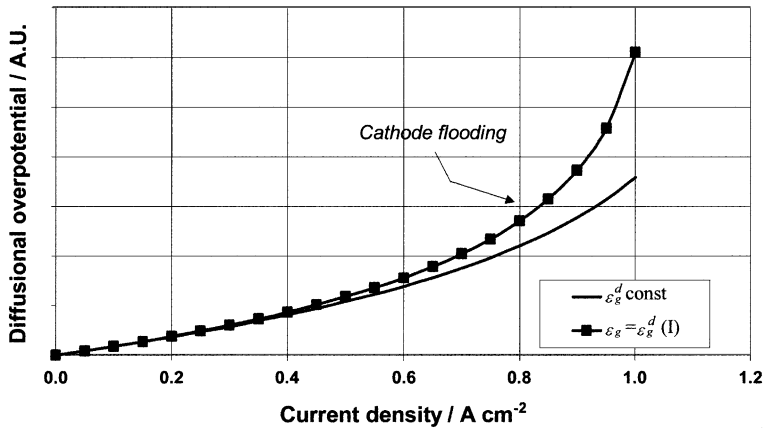

Fig. 2. Qualitative effect of cathode flooding on diffusional overpotential, based on Eqs. (26), (31) and (32).

electro-osmosis could not be sufficient to avoid dehydration on the cathode side of the membrane.

Another innovative element of the proposed model is represented by Eq. (27) used to calculate the diffusional overpotential, which is partly based on some modeling approaches of semi-empirical type [16,34]. In fact, the relationship commonly reported in literature [30,31] in this respect is very general, and does not seem to provide a good description of the diffusional problems at high current densities: the diffusional overpotential of the PEFC results underestimated. Some models proposed for PEFCs are not able to provide an adequate description of the cell behavior in the whole range of current densities [12,13]. In fact, they often result approximate in the high current density region, just where the diffusional overpotentials (mass-transport problems) prevail, especially when air is used as reactant gas. On the contrary, the innovative elements introduced in our model allowed to obtain an excellent agreement with the experimental results of a polymer fuel cell.

4. Model input data

The proposed model has been validated through application to polymer fuel cells with a Nafion 117 membrane, whose experimental results coming from our laboratory are available. Afterwards, on the basis of literature data, the model has also been applied to a fuel cell based on a Dow membrane in order to make a comparison between the two membranes.

Table 1
Input data relative to the cell and the electrodes

Datum	Value
Current densities (A cm^{-2})	$0.5 \times 10^{-3} \div 0.850$[a]
Cell temperature (°C)	70[a] (base-case)
Electrode surface (cm^2)	50[a]
Electrode gas-diffusion layer thickness (μm)	360[a]
Electrode hydraulic permeability (cm^2)	4.73×10^{-15} [1]
Cathode feed gas	Air[a]
Anode gas pressure (atm)	2.5[a] (base-case)
Cathode gas pressure (atm)	3.0[a] (base-case)
Anode inlet gas-flow rate (Nl min^{-1})	0.53[a]
Cathode inlet gas-flow rate (Nl min^{-1})	3.0[a]
Anode humidifying temperature (°C)	85[a] (base-case)
Cathode humidifying temperature (°C)	75[a] (base-case)

[a] Experimental data CNR-ITAE.

The input data are summarized in Tables 1–3. As regards the parameters required for electrochemical calculations listed in Table 2, the initial porosity of the gas-diffusion

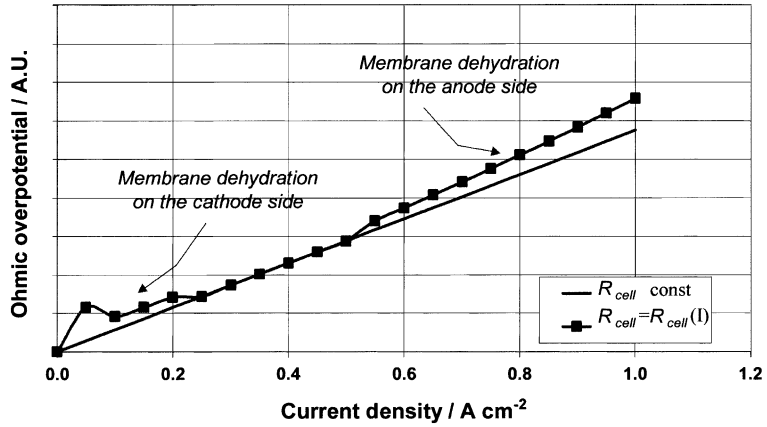

Fig. 3. Qualitative effect of membrane dehydration on ohmic overpotential, based on Eqs. (25), (30) and (33).

Table 2
Input data required for electrochemical calculations

Datum	Value
Initial gas porosity in gas-diffusion layer (%)	30[a]
Catalyst surface area ($cm^2\ mg^{-1}$)	1100[a]
Catalyst loading ($mg\ cm^{-2}$)	0.15[a]
Catalyst utilization	0.5[a]
Exchange current density per Pt surface ($A\ cm^{-2}$)	6.0×10^{-9} (Nafion 117)[b]; 6.6×10^{-9} (Dow)[c]
Membrane resistance/cell resistance ratio	0.77[d]
Empirical constant for diffusional overpotential ($\Omega\ cm^2\ K^{-1}$)	3.4×10^{-4}[e]
Water amount for complete flooding ($mol\ s^{-1}$)	3.0×10^{-3}[f]

[a] Experimental data CNR-ITAE.
[b] This value comes from elaboration of experimental cell potential by a program developed with the software package Mathematica™ [35].
[c] From data reported in [36]: the ratio between the exchange current densities Dow/Nafion 117 is about 1.1 at 70°C and cathode pressure 3 atm.
[d] From experimental measurements carried out at CNR-ITAE, a membrane resistance (Nafion 117) of $0.16 \pm 0.02\ \Omega\ cm^2$ results, and the global cell resistance $= 0.20 \pm 0.02\ \Omega\ cm^2$ in the intermediate current densities region.
[e] From extrapolation of data reported in [34].
[f] This value is fixed so as to have about a 10% increase in resistance from 0 to 0.8 $A\ cm^{-2}$, in agreement with data reported in [26].

Table 3
Membrane properties required as input data

Property	Nafion 117, 7 mil	Dow, 7 mil
Wet thickness (μm)	230 [1,37]	230 [37]
Dry density ($g\ cm^{-3}$)	1.84 [38]	2.143[a]
Equivalent weight ($g\ mol^{-1}$)	1100 [36,38]	800 [36]
Hydraulic permeability (cm^2)	1.8×10^{-14} [1]	1.8×10^{-14} [1]
Average pore diameter (Å)	55 [1,37]	44 [1,37]
Water porosity (%)	28 [1,37]	44 [1,37]
H^+ diffusion coefficient at 22°C ($cm^2\ s^{-1}$)	1.4×10^{-5} [27]	2.0×10^{-5} [27]

[a] This value is derived from Eq. (1), based on a fixed-charge concentration of 1.5×10^{-3} $mol\ cm^{-3}$ [1], and on the porosity and equivalent weight values reported in the table.

layer and the data relative to the catalyst refer to electrodes manufactured in house; the other parameters ($I_{o,Pt}$, τ_R, ω, and $M_{1,max}$) have been determined according to the specifications accompanying the table. In general, when the experimental data of cell potential are available, these model parameters are ''fitting parameters'', which allow to adjust the behavior of the theoretical curve. The exchange current density per Pt surface ($I_{o,Pt}$) influences the low current density region controlled by activation. The ratio between membrane and cell resistance (τ_R) influences the intermediate current density region, where the ohmic overpotentials prevail. The empirical constant ω and the water amount corresponding to a complete flooding ($M_{1,max}$) influence the high current density region, dominated by diffusional problems; even if, on the basis of assumption (34), the parameter $M_{1,max}$ partly conditions the ohmic losses.

It must be observed that, apart from the value of exchange current density per Pt surface, the values required for electrochemical calculations (Table 2) have been assumed to be equal for the two membranes, as a first approximation. Nevertheless, such a hypothesis should be better verified in further investigations.

For the membrane properties (Table 3), we made reference to literature data [1,27,36–38] relative to 7 mil (~175 μm) thick membranes in the dry, H^+ state.

5. Results and discussion

The properties calculated by the model for the two membranes considered are reported in Table 4. The comparison shows that some properties (saturated vapor pressure, water viscosity and density), depending only on the temperature of membrane operation (70°C in this case), have the same value for both membranes.

The electrokinetic permeabilities of the two membranes, calculated by Eq. (2), are also equal; but in such a case, this result comes from a balance between the volume of the membrane pores and their size. In fact, the Dow membrane

Table 4
Membrane properties calculated at 70°C

Property	Nafion 117, 7 mil	Dow, 7 mil
Saturated vapor pressure (atm)	0.3046	0.3046
Pore-water viscosity ($kg\ m^{-1}\ s^{-1}$)	4.04×10^{-4}	4.04×10^{-4}
Pore-water density ($mol\ cm^{-3}$)	0.0543	0.0543
H^+ diffusion coefficient ($cm^2\ s^{-1}$)	3.8×10^{-5}	5.5×10^{-5}
Initial ionic conductivity ($\Omega^{-1}\ cm^{-1}$)	0.151	0.269
Fixed-charge concentration ($mol\ cm^{-3}$)	1.2×10^{-3}	1.5×10^{-3}
Electrokinetic permeability (cm^2)	1.06×10^{-15}	1.06×10^{-15}

is characterized by a larger porosity (44 versus 28%), but it has a lower pore diameter (44 versus 55 Å). Other membrane characteristics calculated by the model show better values for Dow, in terms of fixed-charge concentration, protonic diffusion, and ionic (initial) conductivity (78% higher than Nafion 117), in agreement with literature [1].

Besides, calculations [39] based on a concentrated solution theory [40] showed that in spite of a higher frictional coefficient between water and polymer, the Dow membrane takes advantage of a reduced friction of the hydrogen ions inside the membrane. This result agrees with some studies [37] that attribute to the Dow membrane, characterized by a high protonic diffusion coefficient (see Table 4), reduced water flow rates, and a better proton transport (compared with Nafion 117).

A substantial difference between the two membranes is represented by the water-transport number (Eq. (14)), whose calculated values for Dow membrane are lower than Nafion 117 (the average difference is 0.31 H_2O/H^+, and lies from a minimum of 0.26 H_2O/H^+ at 0.250 A cm^{-2} to a maximum of 8.04 H_2O/H^+ at OCV), in agreement with literature [41,42]. This difference leads to different water requirements (M_- and M_+) to achieve water balance conditions. So that, in any case, the flooding and/or dehydration problems will be more significant for the fuel cell based on Nafion 117 membrane.

In Figs. 4–9, the model results corresponding to the electrochemical calculations are presented. In particular, Fig. 4 shows the behavior of diffusional and ohmic overpotential calculated for the fuel cell based on Nafion 117

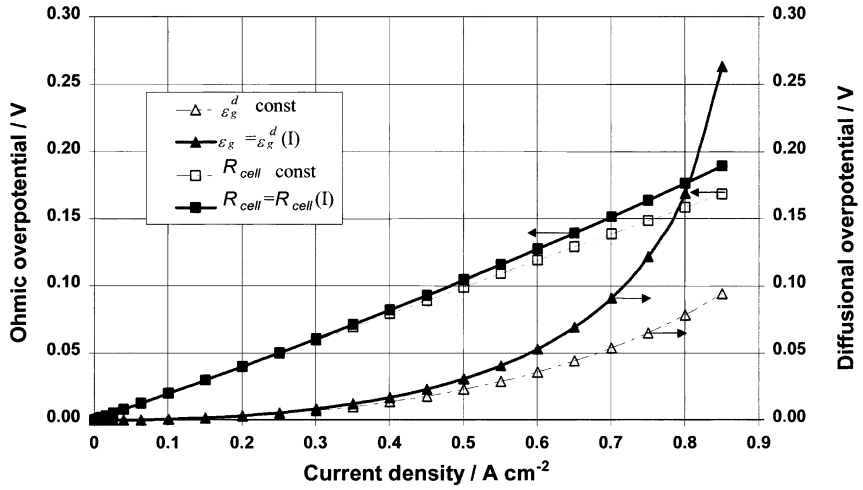

Fig. 4. Influence of flooding and dehydration problems on diffusional and ohmic overpotentials calculated by the model in the case of a Nafion 117 membrane.

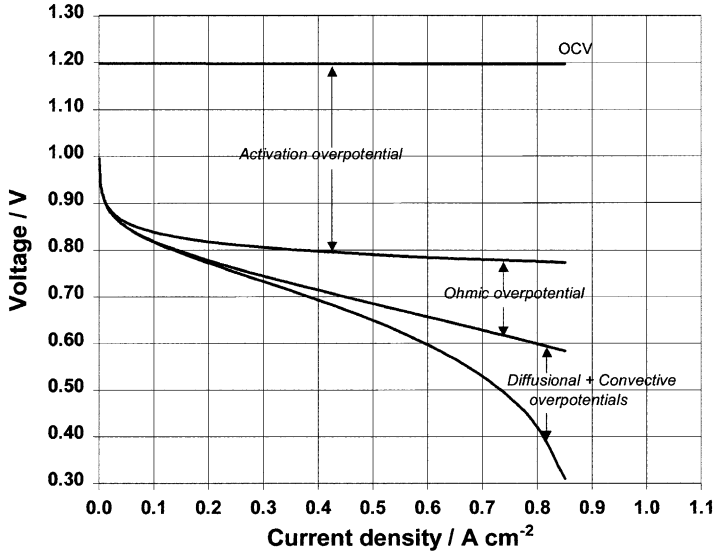

Fig. 5. Overpotential contributions calculated by the model in the case of a Nafion 117 membrane.

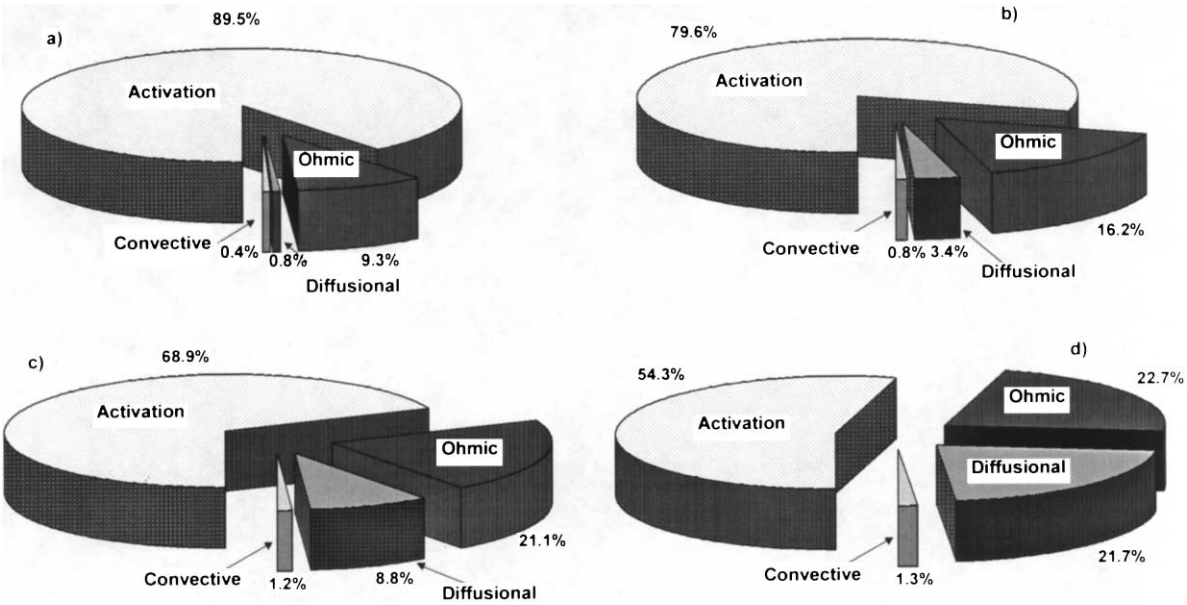

Fig. 6. Percentage of overpotential contributions calculated for Nafion 117 membrane at four current density values: (a) 0.2 A cm^{-2}; (b) 0.4 A cm^{-2}; (c) 0.6 A cm^{-2}; (d) 0.8 A cm^{-2}.

membrane (base-case), according to two different hypotheses: in the absence of flooding (ε_g^d constant: 30%) and dehydration phenomena (R_{cell} constant: 0.198 $\Omega\,cm^2$), and in the presence of such problems (ε_g^d and R_{cell} vary with current density). In compliance with the expectations anticipated in Figs. 2 and 3, it can be observed that the diffusional overpotential is enhanced by the flooding problems of the cathode gas-diffusion layer, going from 0.094 V (in the absence of flooding) to 0.263 V at 0.850 A cm^{-2}. Analogously, the ohmic overpotential suffers from the dehydration of the anode side of the membrane; in fact, it increases from 0.168 to 0.189 V at 0.850 A cm^{-2}. Vice versa, there is no evidence of any dehydration of the cathode side of the membrane (possible, sometimes, at low current densities); but this is justified by the humidification conditions chosen.

As already mentioned, the behaviors presented in Fig. 4 are due to the two negative effects: a decrease, caused by flooding of the gas porosity in the diffusional layer; an increase, caused by dehydration of the overall cell resistance. In fact, the gas porosity passes from the initial 30% (at OCV) to 22.7% (~24% less!) at 0.850 A cm^{-2}; while, the cell resistance goes from 0.198 $\Omega\,cm^2$ (at OCV) to 0.222 $\Omega\,cm^2$ at 0.850 A cm^{-2}, with a rise of about 11%. As Fig. 4 reveals, both these effects become evident (>5 mV) only for current densities larger than about 0.5 A cm^{-2}.

It must be observed that the value of the (initial) ionic conductivity calculated by Eq. (6) allows to obtain (Eq. (30))

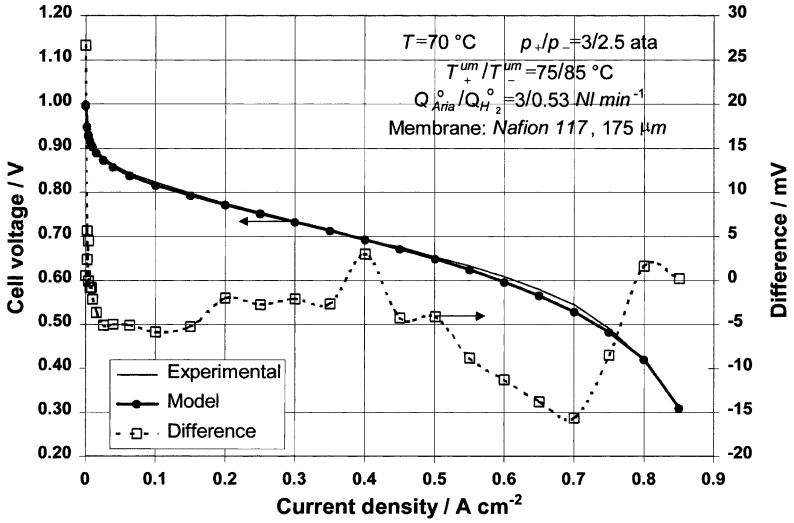

Fig. 7. Polarization curves: comparison between model and experimental results for the base-case of Nafion 117 membrane.

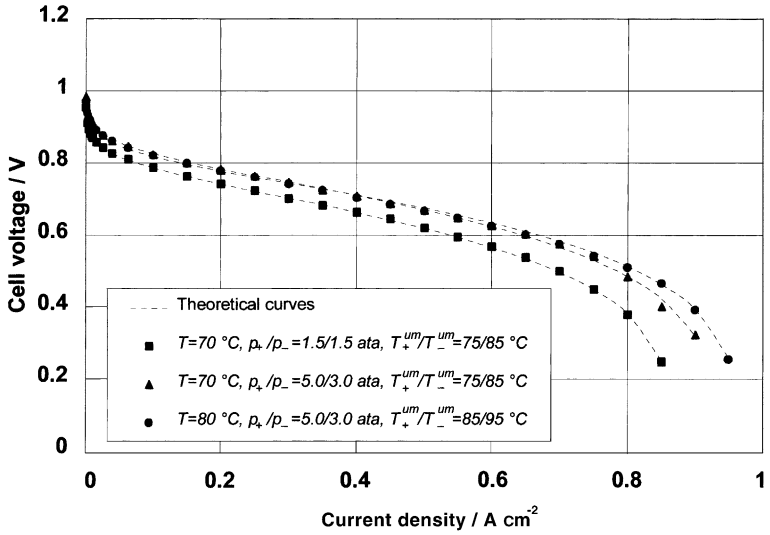

Fig. 8. Comparison between experimental (bullets) and theoretical (dashed lines) polarization curves under different operative conditions (Nafion 117 membrane).

an overall cell resistance (0.204 $\Omega\,cm^2$ at 0.4 A cm^{-2}) in excellent agreement with the value measured in the intermediate current density region, equal to $0.20 \pm 0.02\ \Omega\,cm^2$. Besides, as it will be shown later, it has not been necessary to artfully change the value of the membrane ionic conductivity to achieve a good fitting of the experimental results. Instead, a conductivity equal to 0.07 $\Omega^{-1}\,cm^{-1}$ at 80°C has been considered in [2] to reach a satisfactory fitting of the polarization experimental curves, even though the value calculated by Eq. (6) was significantly higher (i.e. 0.17 $\Omega^{-1}\,cm^{-1}$).

From Fig. 5, it is possible to distinguish the different overpotential contributions calculated by the model for the fuel cell based on Nafion 117 membrane. At low current densities (<0.1 A cm^{-2}), the activation overpotential is almost entirely responsible for the cell voltage losses. For current densities > 0.3 A cm^{-2}, the ohmic losses due to the membrane and the electrodes become more important, and the activation overpotential reaches a relatively constant value. The results also show the effect due to the oxygen mass-transport limitations, which involve an enhanced diffusional overpotential for current densities > 0.6 A cm^{-2}. The overpotential due to proton convection, which in Fig. 5 is coupled to the diffusional overpotential, is not noticeable: it reaches a maximum of 11.2 mV at 0.850 A cm^{-2}.

A fundamental difference, compared with analogous results presented in literature [1,3,4], is an appreciable limitation due to mass-transport phenomena. Actually, in [1,3,4], the only parameter which influences the high current density region is the gas porosity in the diffusional layer ε_g^d, but this is a datum of the model and does not vary with current density. Two extreme cases were presented in [1,3,4]: when the porosity $\varepsilon_g^d = 50\%$, no transport limitations were observed; for $\varepsilon_g^d = 11\%$ instead, the diffusional

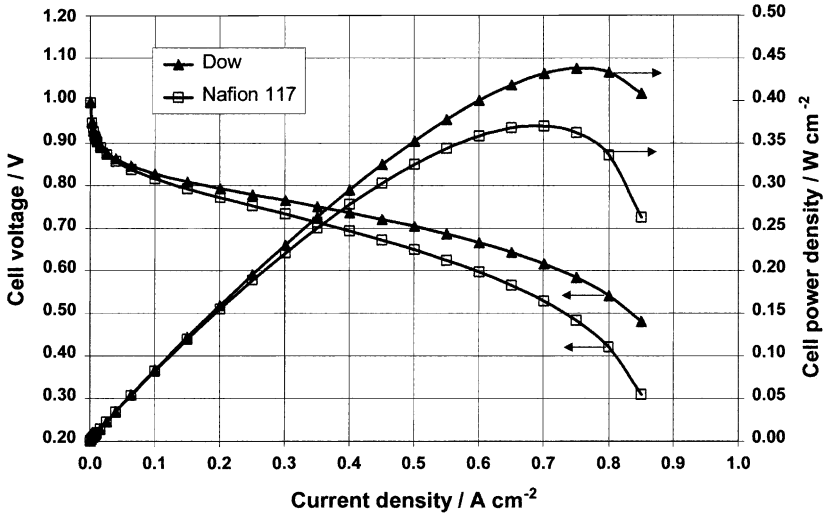

Fig. 9. Polarization and power density curves calculated by the model: comparison between results relative to Nafion 117 (base-case) and Dow membranes.

problems become evident, and the oxygen-limiting current density reaches 0.750 A cm^{-2}. However, the potential drop related to the mass-transport problems appears to be too sharp (the cell voltage is still very high, i.e. about 0.660 V at 0.650 A cm^{-2}) compared with our predictions (Figs. 5–7).

Fig. 6 allows to discern the relative share of the calculated overpotential contributions corresponding to four current density values. The activation overpotential is 89.5% of the total irreversibilities at 0.2 A cm^{-2}, but decreases at 54.3% for 0.8 A cm^{-2}; the percentages of the other contributions, instead, increases with current density. Thus, at 0.8 A cm^{-2}, ohmic and diffusional overpotential both represent more than 21% of the total losses, while convective overpotential does not exceed 1.3%. Is it significant that for constant gas porosity and membrane ionic conductivity, the percentages at 0.8 A cm^{-2} become: 63.2% activation, 23.8% ohmic, 11.8% diffusional, and 1.2% convective overpotential.

Fig. 7 shows the comparison between the model and the experimental results of the fuel cell based on a Nafion 117 membrane. The agreement obtained between the polarization curve predicted by the simulation model and the experimental curve is very satisfactory. In fact, the mean error is in the order of ±5.7 mV, with two relative maxima of +26.6 mV at 0.5×10^{-3} A cm^{-2} (corresponding to +2.8%) and of −15.6 mV at 0.7 A cm^{-2} (equal to −2.9%). Thus, the maximum error for the entire curve is less than ±3%. Moreover, leaving out the first point (0.5×10^{-3} A cm^{-2}) for which there are unquestionable measurement difficulties (recorded values for five experimental curves range from 0.968 to 0.981 V!), the mean error between the two curves reduces to ±4.8 mV; i.e. in percentage terms, ±0.7%. From a more general point of view, apart from few points (0.5×10^{-3}, 2.5×10^{-3}, 0.400, 0.800, and 0.850 A cm^{-2}), it can be noticed that the calculated cell voltage is always slightly lower than the experimental one. However, peculiar behaviors of the error corresponding to the three current density regions controlled by activation, ohmic, and diffusional overpotentials are not observed. Then, as a matter of fact, these three contributions seem to be described with a good accuracy by the mathematical model here proposed, whose validation has been consequently attained.

In fact, further simulations carried out at different operative conditions confirmed the good agreement between the model and the experimental results (Fig. 8).

Fig. 9 shows a comparison of the polarization and power density curves calculated by the model for a fuel cell having the same characteristics of the base-case, with the two different types of membranes. The results, obtained by considering the data reported in Tables 1–3, show a superior performance for the Dow-based fuel cell. Such a performance is justified by several factors that can be easily understood by comparing the overpotential values calculated at 0.850 A cm^{-2} for the two cases (Table 5).

In fact, the higher exchange current density associated with the Dow-based fuel cell, owing to its higher protonic concentration, implies a slightly lower activation overpotential (∼3 mV less in all the current density range). Moreover, the higher protonic concentration of the Dow membrane results in a reduced overpotential for protonic convection: about 8 mV less at 0.850 A cm^{-2}. But, what makes the big difference between the two fuel cells are the ohmic and the diffusional overpotentials, respectively, 88 and 72 mV less at 0.850 A cm^{-2} for the Dow-based fuel cell. Thus, altogether the cell voltage calculated at 0.850 A cm^{-2} results a good 0.171 V higher for the case of the fuel cell with Dow membrane: 0.480 V against 0.309 V for the Nafion-based cell.

Table 5
Comparison between calculated overpotentials at 0.850 A cm^{-2}

Overpotential	Cell with Nafion 117 membrane (mV)	Cell with Dow membrane (mV)	Difference (mV)
Activation	424.33	421.52	2.81
ohmic	189.21	101.31	87.90
Diffusional	263.36	190.92	72.44
Convective	11.15	3.26	7.89

This is clearly due to a lower cell (initial) resistance (0.111 Ω cm^2 against 0.198 Ω cm^2 at OCV), i.e. a higher ionic conductivity of the Dow membrane, but also, in particular, to a less-pronounced effect of the dehydration and flooding problems. In fact, the resistance undergoes an increase equal to 6.7%, and the gas porosity in the diffusional layer suffers a decrease equal to 19.8%, when we pass from OCV to 0.850 A cm^{-2}, versus 11.1 and 24.2%, respectively, for the Nafion-based fuel cell.

This is also related to the values of the water-transport number (Eq. (14)), which in the case of the Dow membrane are lower than those of the Nafion 117 membrane (e.g. 0.67 H_2O/H^+ versus 0.97 H_2O/H^+ at 0.850 A cm^{-2}). Thus, the water transport for electro-osmosis through the Dow membrane is slower, and it contributes to simultaneously reduce the membrane dehydration (at the anode interface) and the cathode flooding.

Obviously, the power density of the fuel cell is also higher for the cell using the Dow membrane, with a maximum of about 0.438 W cm^{-2} at 0.750 A cm^{-2}; whereas, for the cell based on the Nafion 117 membrane, the maximum power density is approximately equal to 0.370 W cm^{-2} at 0.700 A cm^{-2}. The results obtained by the model are, from a qualitative point of view, in agreement with literature [1,3,4,14,21,26], where experimental and/or theoretical polarization curves of PEFCs based on Nafion 117 and Dow membranes are presented, with a clear superior performance for the latter.

6. Conclusions

In this paper, a mathematical model for polymer fuel cells is described; it represents an innovative approach compared

with others reported in literature. In fact, it is based on the introduction of some original relationships that envisage a decrease in the cell resistance and in the porosity available for the gas in the electrode, respectively, due to dehydration on the anode side of the membrane and to cathode flooding. Once the operative conditions are fixed, such relationships allow to determine the ohmic and diffusional overpotentials as a function of the water balance conditions of the fuel cell. The cell voltage is accordingly calculated.

The model results here presented, for the case of a polymer fuel cell using a Nafion 117 membrane, demonstrate an excellent agreement with the experimental voltage values of a cell realized at the CNR-TAE Institute: the maximum error is less than $\pm 3\%$. The simulations carried out at different operative conditions confirm this agreement.

Moreover, a superior performance (0.480 V against 0.309 V at 0.850 A cm^{-2}) was predicted in the case of a fuel cell, with the same characteristics (electrodes, operative, and humidification conditions) based on a Dow membrane, whose relative flooding and dehydration problems are less critical.

In conclusion, the developed model represents a suitable theoretical tool to provide a valid support for an advanced design of the membrane/electrode assembly of PEFCs for the realization of polymeric membranes at low cost and for the optimization of cell-operating conditions.

References

[1] D.M. Bernardi, M.W. Verbrugge, General Motors Report GMR-7360, 15 May 1991.
[2] D.M. Bernardi, M.W. Verbrugge, AIChE J. 37 (1991) 1151–1163.
[3] D.M. Bernardi, M.W. Verbrugge, in: R.E. White, M.W. Verbrugge, J.F. Stockel (Eds.), Proceedings of the Symposium on Modeling of Batteries and Fuel Cells, Vol. 91-10, The Electrochemical Society, Pennington, NJ, 1991, pp. 240–280.
[4] D.M. Bernardi, M.W. Verbrugge, J. Electrochem. Soc. 139 (1992) 2477–2491.
[5] D.M. Bernardi, J. Electrochem. Soc. 137 (1990) 3344–3350.
[6] T.E. Springer, S. Gottesfeld, in: R.E. White, M.W. Verbrugge, J.F. Stockel (Eds.), Proceedings of the Symposium on Modeling of Batteries and Fuel Cells, Vol. 91-10, The Electrochemical Society, Pennington, NJ, 1991, pp. 197–208.
[7] T.E. Springer, T.A. Zawodzinski, S. Gottesfeld, in: R.E. White, M.W. Verbrugge, J.F. Stockel (Eds.), Proceedings of the Symposium on Modeling of Batteries and Fuel Cells, Vol. 91-10, The Electrochemical Society, Pennington, NJ, 1991, pp. 209–229.
[8] M.S. Wilson, T.E. Springer, T.A. Zawodzinski, S. Gottesfeld, in: Proceedings of the 26th Intersociety Energy Conversion Engineering Conference, Vol. 3, Boston, 4–9 August 1991, pp. 636–641.
[9] T.E. Springer, T.A. Zawodzinski, S. Gottesfeld, J. Electrochem. Soc. 138 (1991) 2334–2342.
[10] T. Springer, S. Gottesfeld, M. Wilson, in: Proceedings of the Fall Meeting of The Electrochemical Society, Toronto, 11–16 October 1992, Abstract 91.
[11] T.E. Springer, M.S. Wilson, S. Gottesfeld, J. Electrochem. Soc. 140 (1993) 3513–3525.
[12] E.A. Ticianelli, C.R. Derouin, A. Redondo, S. Srinivasan, in: S. Srinivasan, S. Wagner, H. Wroblowa (Eds.), Proceedings of the Second Symposium on Electrode Materials and Processes for Energy Conversion and Storage, Vol. 87-12, The Electrochemical Society, Pennington, NJ, 1987, pp. 166–181.
[13] E.A. Ticianelli, C.R. Derouin, A. Redondo, S. Srinivasan, J. Electrochem. Soc. 135 (1988) 2209–2214.
[14] S. Srinivasan, D.J. Manko, H. Koch, M.A. Enayetullah, A.J. Appleby, J. Power Sources 29 (1990) 367–387.
[15] E.A. Ticianelli, J. Electroanal. Chem. 387 (1995) 1–10.
[16] J. Kim, S.-M. Lee, S. Srinivasan, C.E. Chamberlin, J. Electrochem. Soc. 142 (1995) 2670–2674.
[17] J.C. Amphlett, M. Farahani, R.F. Mann, B.A. Peppley, P.R. Roberge, in: Proceedings of the 26th Intersociety Energy Conversion Engineering Conference, Vol. 3, Boston, 4–9 August 1991, pp. 624–629.
[18] J.C. Amphlett, R.M. Baumert, R.F. Mann, B.A. Peppley, P.R. Roberge, T.J. Harris, J. Electrochem. Soc. 142 (1995) 1–8.
[19] J.C. Amphlett, R.M. Baumert, R.F. Mann, B.A. Peppley, P.R. Roberge, T.J. Harris, J. Electrochem. Soc. 142 (1995) 9–15.
[20] S.J. Ridge, R.E. White, Y. Tsou, R.N. Beaver, G.A. Eisman, J. Electrochem. Soc. 136 (1989) 1902–1909.
[21] A. Cisar, in: Proceedings of the 26th Intersociety Energy Conversion Engineering Conference, Vol. 3, Boston, 4–9 August 1991, pp. 611–618.
[22] M.C. Kimble, N.E. Vanderborgh, in: Proceedings of the 27th Intersociety Energy Conversion Engineering Conference, Vol. 3, San Diego, 3–7 August 1992, pp. 413–417.
[23] J.D. Canaday, T.A. Wheat, A.K. Kuriakose, A. Ahmad, Int. J. Hydrogen Energy 12 (1987) 151–157.
[24] J.-T. Wang, R.F. Savinell, Electrochim. Acta 37 (1992) 2737–2745.
[25] X. Yu, R. Zhang, J.M. Fenton, in: Proceedings of the Spring Meeting of The Electrochemical Society, Honolulu, 16–21 May 1993, Abstract 1304.
[26] M.S. Wilson, J.A. Valerio, S. Gottesfeld, Electrochim. Acta 40 (1995) 355–363.
[27] A.G. Guzman-Garcia, P.N. Pintauro, M.W. Verbrugge, E.W. Schneider, J. Appl. Electrochem. 22 (1992) 204–214.
[28] R.C. Weast (Ed.), Handbook of Chemistry and Physics, 62nd Edition, CRC Press, Boca Raton, 1981–82, Section F, pp. 11–42.
[29] P. Staiti, Z. Poltarzewski, V. Alderucci, G. Maggio, N. Giordano, J. Appl. Electrochem. 22 (1992) 663–667.
[30] K. Kinoshita, F.R. McLarnon, E.J. Cairns, Fuel Cells — A Handbook, prepared by Lawrence Berkeley Laboratory for the US Department of Energy under contract no. DE-AC03-76SF00098, May 1988.
[31] J.H. Hirschenhofer, D.B. Stauffer, R.R. Engleman, Fuel Cells — A Handbook (Revision 3), prepared by Gilbert/Commonwealth Inc. for the US Department of Energy under contract no. DE-AC01-88FE61684, January 1994.
[32] M.W. Verbrugge, R.F. Hill, J. Electrochem. Soc. 137 (1990) 886–893.
[33] J. Leddy, N.E. Vanderborgh, Los Alamos National Laboratory Report LA-UR 86-2072, 1986.
[34] G. Squadrito, G. Maggio, E. Passalacqua, F. Lufrano, A. Patti, J. Appl. Electrochem. 29 (1999) 1449–1455.
[35] A.S. Aricò, A.K. Shukla, V. Antonucci, N. Giordano, J. Power Sources 50 (1994) 177–186.
[36] M. Wakizoe, O.A. Velev, S. Srinivasan, Electrochim. Acta 40 (1995) 335–344.
[37] M.W. Verbrugge, R.F. Hill, J. Electrochem. Soc. 137 (1990) 3770–3777.
[38] M.W. Verbrugge, R.F. Hill, J. Phys. Chem. 92 (1988) 6778–6783.
[39] G. Maggio, V. Recupero, L. Pino, CNR-ITAE Report no. 14/98, September 1998.
[40] T.F. Fuller, J. Newman, in: R.E. White, A.J. Appleby (Eds.), Proceedings of the Symposium on Fuel Cells, Vol. 89-14, The Electrochemical Society, Pennington, NJ, 1989, pp. 25–38.
[41] N.E. Vanderborgh, M.C. Kimble, J.R. Huff, J.C. Hedstrom, in: Proceedings of the 27th Intersociety Energy Conversion Engineering Conference, Vol. 3, San Diego, 3–7 August 1992, pp. 407–411.
[42] T.A. Zawodzinski Jr., T.E. Springer, J. Davey, R. Jestel, C. Lopez, J. Valerio, S. Gottesfeld, J. Electrochem. Soc. 140 (1993) 1981–1985.